The Adaptive Optics System of the 1.5m GREGOR Solar Telescope - four years of operation

Thomas Berkefeld[1], Dirk Schmidt[2], Dirk Soltau[1], Frank Heidecke[1], and Andreas Fischer[1]

[1]Kiepenheuer-Institut für Sonnenphysik, Schöneckstr. 6, 79104 Freiburg, Germany
[2]National Solar Observatory, 3665 Discovery Drive, Boulder, CO 80303, USA

ABSTRACT

We present the properties of the adaptive optics (AO) system of the German 1.5m solar telescope GREGOR, located on the island of Tenerife, Spain. The conventional AO system uses a correlating Shack-Hartmann-Sensor with a 92 mm subaperture size and a 256-actuator stacked-piezo deformable mirror (DM). AO performance results and practical experience based on the last four years of operation are presented. A recently installed second wavefront sensor with exchangeable lenslets / subaperture sizes in combination with an EM-CCD camera is used for low light observations such as polarimetric measurements of the solar system planets. Further developments include algorithmic improvements, the use of the night-time sensor for solar (off-limb) observations and solar MCAO.

1. INTRODUCTION

For many years now, Adaptive Optics has been a mature and indispensable technology at solar telescopes to conduct observations at high spatial resolution. In contrast to night-time AO systems whose point sources

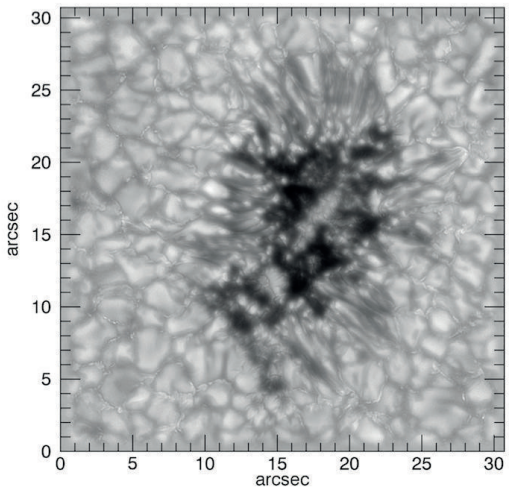

Figure 1. Sunspot and surrounding granulation as examples of solar surface details at 600 nm. The image has been post-processed with speckle techniques and provides a resolution of 0.1 arcsec (diffraction-limited).

used as WFS targets are obviously much smaller than the isoplanatic patch, solar AO systems have to rely on correlating Shack-Hartmann sensors whose typical field of view of 10"-12" exceeds the isoplanatic patch in the visible. Therefore solar AO systems have a bit of the characteristics of a ground layer AO in the sense that they correct a FoV that is larger than the isoplanatic patch but do not quite reach high Strehl. Due to the dependance on the C_n^2-profile, no single Strehl number for a given r_0 can express the performance. Nevertheless solar AO - as night-time AO - drastically improves the image quality. Especially useful is the combination of

Send correspondence to Thomas Berkefeld, E-mail: tberkefeld@leibniz-kis.de

Adaptive Optics Systems V, edited by Enrico Marchetti, Laird M. Close, Jean-Pierre Véran, Proc. of SPIE Vol. 9909, 990924
 · doi: 10.1117/12.2232604

AO and postprocessing / image reconstruction techniques such as phase diversity,[1] speckle reconstruction[2,3] or MOMFBD (Multi-Object Multi Frame Blind Deconvolution)[4] which benefit from the much increased signal to noise ratio (SNR) provided by the AO.

The 1.5 m German solar telescope GREGOR was built to conduct solar observations at high spatial, spectral and polarimetric resolution. It has been equipped a with high order AO system almost from the beginning. Fig.

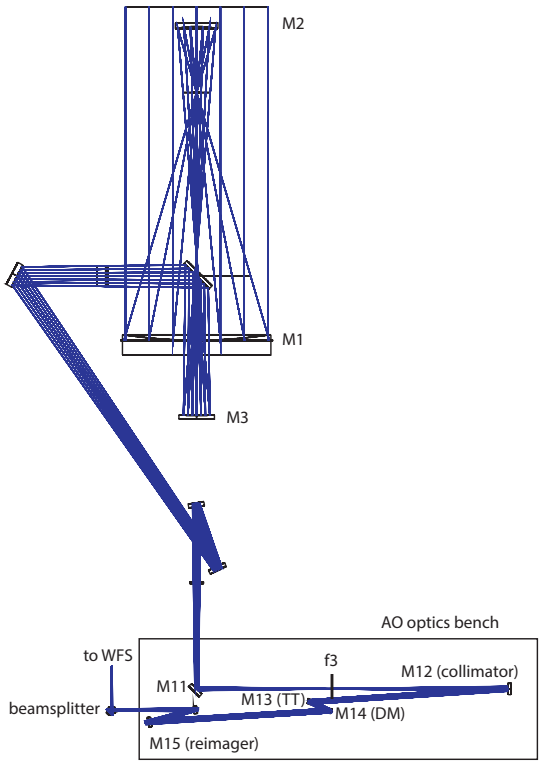

Figure 2. GREGOR optics scheme

2 shows the optics design: GREGOR is a double Gregory-type telescope with the prime focus limiting the FoV to 150 arcsec and the downstream heat load to less than one percent of the original heat load. The secondary focus is in the rotationally symmetric part of the optics and contains a polarimetric calibration unit. The tertiary mirror M3 generates the final f/40 beam. M11, being close to the focus, is used to center the pupil on the DM by utilizing the intensity information of the WFS' edge subapertures. The AO setup itself is a typical AO relay consisting of collimator, tip-tilt mirror, DM and reimager. The WFS pickoff is close the science focus, keeping the non-common path aberrations (NCPA) low.

2. SOLAR AO

Table 1 lists the basic parameters of the GREGOR solar AO.

The operational regimes are not limited by the stroke of the DM (except for bad seeing > 2.5") but by the signal to noise ratio (SNR) of the correlating Shack-Hartmann WFS. According to Michau,[5] the measurement error for a critically sampled correlating single aperture and an extended target such as granulation is

$$\sigma^2_{\mathrm{snr}} = \frac{20\sigma^2_{\mathrm{noise}}}{n^2\sigma^2_{\mathrm{signal}}} \qquad [\lambda^2], \tag{1}$$

where σ_{noise} denotes the rms noise level (mostly photon noise), n the number of pixels across the cross-correlation field of view (24) and $\sigma_{\mathrm{signal}}/I_{\mathrm{mean}}$ the image contrast (typically a few percent for granulation). The equation

Table 1. Basic parameters of the GREGOR solar AO. The DM is also used for the night-time AO. Due to the exchange of the secondary mirror in late 2016, we expect to see an improved contrast transfer inside the telescope in 2017 and thus improved WFS locking capabilities similar to the Vacuum Tower Telescope, Tenerife

seeing: operational regime (sunspots)	<2.5"
seeing: operational regime (pores)	<1"-2" (now), <2.5" (from 2017)
seeing: operational regime (granulation)	<0.7" (now), <1.5" (from 2017)
min. distance to solar limb (lock on faculae pts)	not possible (now), <1.5" (from 2017)
deformable mirror	stacked piezo, 256 actuators (CILAS)
number of subapertures	156 (15 across, Fried geometry)
WFS correlation FoV / # pixels per correlation	12" / 24x24
number of corrected modes	up to 152 KL/ 180 opt. basis
control loop frequency	2100 Hz
0-db bandwidth	max. 110 Hz

shows that high quality optics (low surface roughness at mid to high spatial frequencies), a high full well capacity and good linearity of the WFS camera and a reasonably-sized correlation field are required for keeping the noise level low. These points are mandatory for achieving a good AO performance when locking on granulation. The intrinsic RMS contrast of 15% at 500 nm is lowered by the atmosphere, the MTF of the subapertures and non-perfect optics down to 2-5% at the WFS camera.

2.1 Data Reduction and Cross-Correlation

We apply the usual standard procedure that is used for solar AO[6] (for each subaperture separately): dark/flatfield correction, removal of intensity gradients across the FoV, application of an apodization window (only if the cross-correlation is computed in Fourier space), and intensity normalization. As crosscorrelation techniques, we use the FFT-based crosscorrelation. Although it is not as accurate as e.g. the square difference function,[7] and tends to underestimate the shift error, it has the advantage of a large dynamic range (the crosscorrelation function is as wide the correlation FoV), which is useful when closing the loop. Furthermore, for small shifts (closed loop), the resulting drop in bandwidth is small.

2.1.1 The Size of the Correlation Field

The 0.76m Dunn Solar Telescope[8] and the future 4m Daniel K. Inouye Solar Telescopedkistao use 20x20 pixels whereas the 0.7m Vacuum Tower Telescope,[9] the 1.5m GREGOR[6] and the 1m New Swedish Solar Telescope[10] use 24x24 pixels. The 1.6m Big Bear Solar Observatory uses 16x16 pixels.[11] A larger FoV of the WFS increases the accuracy of the crosscorrelation and the corrected science FoV but reduces the peak Strehl at the center of the FoV and requires faster WFS cameras. We found 24x24 pixels to work well for the typical C_n^2-profil on Tenerife.

A reasonable size of the crosscorrelation field also depends on the full well capacity and the linearity of the WFS camera and, for on-axis telescopes, on the thickness of the telescope spiders, which all affect the SNR. The obstruction by the support spiders causes a decrease of the contrast in the affected subapertures. Therefore the spiders must be kept as thin as possible. Completely obstructed subapertures rows/columns at large telescopes can cause phasing problems that must be dealt with in the reconstructor.[12]

2.2 Wavefront Reconstruction, Servo

We use a two-step reconstructor from shifts-to-modes and modes-to actuators. The modal basis is either a set of 152 Karhunen-Loeve modes projected on the DM or a set of 180 optimal basis modes. Since there is almost no performance difference, we usually use the KL-modes. A modal gain optimizer helps to minimize the residual modal errors by maximizing the modal error attenuation factor. The servo is a leaky PI controller. Although it works quite well, it does not help much do reduce vibration effects due to their relatively high frequencies. We therefore plan to add a predictor element to our tip-tilt servo loop.

As an example, Fig. 3 shows the modal RMS error [rad] at 500nm as a function of the mode number for a set of 180 optimal basis modes before and after correction when the GREGOR AO was locked on a sunspot. Only dynamic errors (atmospheric turbulence, vibrations) are included. It can be seen that the residual tip-tilt (mainly vibrations in the f1 heat stop cooling system) and astigmatism (vibrations in the M1 cooling system) errors are particularly high.

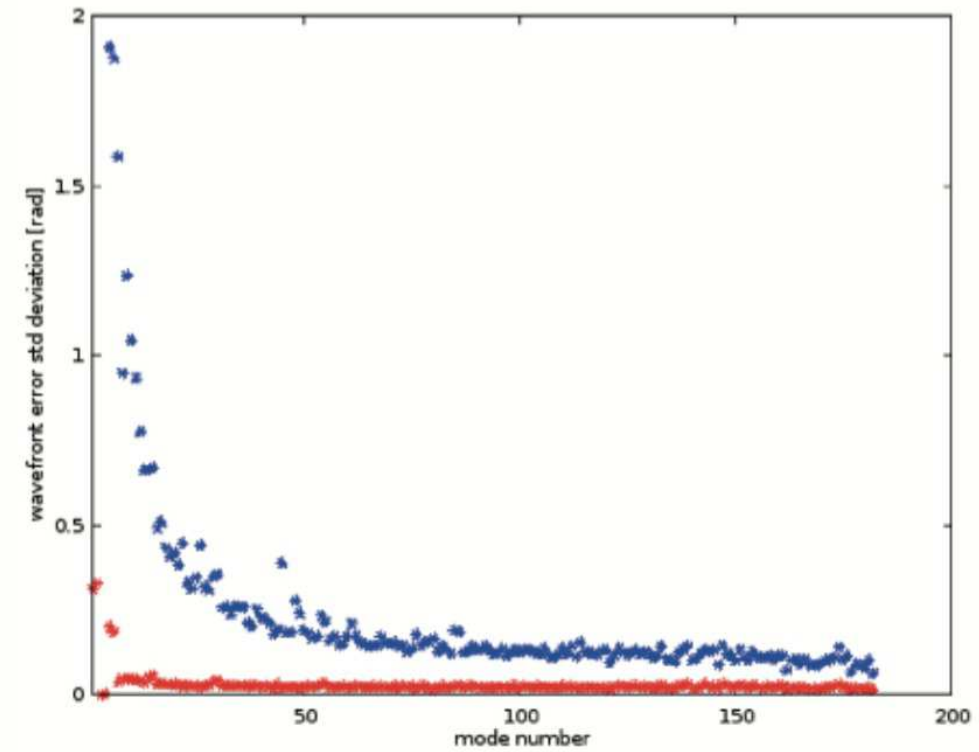

Figure 3. modal standard deviation (static errors removed) at 500nm before (blue) and after (red) correction

2.3 Hardware, Software

Wherever possible, we use off-the-shelf components. This includes the control computer, WFS camera, interface boards etc. Using CPU-based computing (no FPGA / DSP / GPUs) has facilitated the development of the AO control software and allows easy integration of new features. Today's multi-core CPU multi-CPU systems are fast enough to drive even large solar (MC)AO systems (some of the MCAO configurations at the Big Bear Solar Telescope have the same system complexity as the DKIST AO.).

The major non off-the-shelf components are the 256-actuator DM made by CILAS and its high voltage amplifier which is an in-house development. As interfaces we use CameraLink for the WFS camera and CameraLink as output to drive the TT and DM (the used CameraLink-to-RS422 converter is also an in-house development).

3. NIGHT-TIME-AO

In order to measure the polarimetric signals of the gas giants as specimen for polarimetric signatures of extra-solar planets,[13] GREGOR is equipped with a night-time correlating SH-WFS. GREGOR has the feature of a polarimetric calibration unit at the secondary focus which is still in the symmetric part of the optics, leading to higher polarimetric accuracy as compared to off-axis telescopes. For adapting to the size, shape and brightness of the target, two lenslets with different geometries can be inserted into the pupil image of the WFS. Since the target can be larger than the FoV of the WFS, a field stop matching the lenslet must be inserted into the entrance focus of the WFS.

Table 2. Basic parameters of the GREGOR night-time AO

deformable mirror	stacked piezo, 256 actuators (CILAS)
WFS type	correlating Shack-Hartmann
number of subapertures	24 or 54 (2 or 3 keystone rings)
approx. limiting magnitude	8 or 6.5
WFS correlation FoV (circular)	10" or 6.5"
# pixels across correlation field	20 or 13
number of corrected modes	up to 30 or 65
control loop frequency	up to 970 Hz
0-db bandwidth	max. 60 Hz

Table 2 lists the different lenslets and the resulting properties.

For measurements of the solar system planets, the 24-subaperture setup was used. So far Venus, Uranus and Neptune have been observed.

GREGOR, as a solar telescope, is not as optimized as a night-time telescope for high light throughput. Furthermore, since a 50/50 beamsplitter divides the light between the science instrument and the WFS (both observe at visible wavelengths), only 10% of the photons entering the telescope create electrons in the WFS camera, limiting the GREGOR night-time AO to relatively bright objects.

The WFS camera is a Nuvu EM-CCD camera with 128x128 pixels. The effective read noise is less than $1e^-$ when used at high EM-gains. The maximum readout frequency is 970 Hz.

For shift determination, center of gravity or square difference function with either predefined- or WFS reference images can be used. The wavefront reconstruction and servo control is the same as in the solar AO case. The modal gain optimizer is even more important than in the solar case: In addition to adapt the gains to the target shape and seeing conditions, it also adjusts according to the target brightness. Presently, adjusting the WFS camera integration time and frequency according to the target brightness has to be done manually.

Figure 4 shows the polarimetric signal of Uranus for three different wavelengths observed with GREGOR and its night-time AO. The polarimetric signature is 2-3%.

4. ONGOING AND FUTURE DEVELOPMENT

After the exchange of the secondary mirror in 2016, the solar WFS (2016) and the night-time WFS (2017) will be relocated on the same optical bench that accommodates the tip-tilt mirror and the DM, thus eliminating the presently frequent misalignments between DM and lenslet. This change will improve the reliability and give a reproducible performance. A performance evaluation of the solar and the night-time AO will be conducted afterwards. The improved capability to lock on granulation will allow us to resume the MCAO experiments (for a detailed description see[14,15]).

In order to reduce the effects of vibrations we plan to add a predictive element to the tip-tilt servo loop. A new WFS flatfielding procedure will eliminate the problem of bad flatfields of the spider-affected subapertures.

As a future solar application, a narrow-band Hα interference filter will allow us to close the night-time AO loop on solar prominences. A first test at GREGOR has shown that this is feasible, however, due to the lower bandwidth and less corrected degrees of freedom of the night-time AO as compared to the solar AO, the performance will be diffraction-limited only in the rare cases of very good daytime seeing. For achieving the typical performance of the solar AO when locking on prominences, low noise cameras with a pixel frequency of about 500 Mpixel/sec are required, but not available.

The GREGOR AO has been the workhorse for the last four years of operation and has been used for more than 90% of the observations. With the improvements and new capabilities described above, the scientific capabilities of GREGOR will become even more diverse.

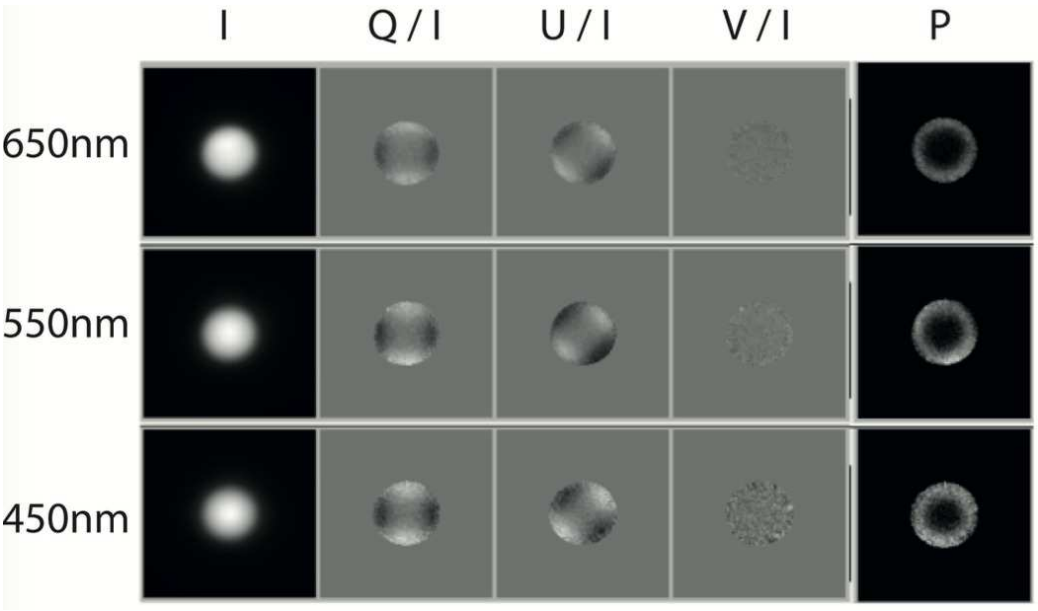

Figure 4. polarimetric signature of Uranus.

A number of KIS co-workers contributed in various forms to the construction, setup and commissioning of the GREGOR Adaptive Optics System. We would particularly like to name and thank A. Bernert, K. Gerber, P. Markus, S. Semeraro, T. Sonner and O. Wiloth.

REFERENCES

[1] van Noort, M., Rouppe van der Voort, L., and Löfdahl, M. G., "Solar image restoration by use of multi-frame blind de-convolution with multiple objects and phase diversity," *Solar Physics, Volume 228, Issue 1-2* , 191–215 (2005).

[2] Lühe, O., "Solar speckle imaging," *High spatial resolution solar observations, Proceedings of the 10th Sacramento Peak Summer Workshop, Sunspot, New Mexico, August 22-26, 1988* , 147ff (1989).

[3] Mikurda, K. and Lühe, O., "High resolution solar speckle imaging with the extended knox thompson algorithm," *Solar Physics, Volume 235, Issue 1-2* , 31–53 (2006).

[4] Tritschler, A. and Schmidt, W., "Sunspot photometry with phase diversity. i. methods and global sunspot parameters," *Astronomy and Astrophysics, v.382* , 1093–1105 (2002).

[5] Michau, V., Rousset, G., and Fontanella, J., "Wavefront Sensing from Extended Sources," *R.R. Radick (ed.), Real Time and Post-Facto Image Correction, NSO/SP Summer Workshop Ser. 13* , 124–127 (1992).

[6] Berkefeld, T., Schmidt, D., Soltau, D., von der Lühe, O., and Heidecke, F., "The GREGOR adaptive optics system," *Astronomische Nachrichten, Vol.333, Issue 9* , 863ff (2012).

[7] Löfdahl, M., "Evaluation of image-shift measurement algorithms for solar Shack-Hartmann wavefront sensors," *Astronomy and Astrophysics, Volume 524, id.A90* , 17ff (2010).

[8] Rimmele, T., "Recent advances in solar adaptive optics," *Proc. SPIE 5490* , 34–46 (2004).

[9] von der Lühe, O., Soltau, D., Berkefeld, T., and Schelenz, T., "KAOS: Adaptive optics system for the Vacuum Tower Telescope at Teide Observatory," *Proc. SPIE 4853* , 187–193 (2003).

[10] Scharmer, G., Bjelksjo, K., Korhonen, T., Lindberg, B., and Petterson, B., "The 1-meter Swedish solar telescope," *Proc. SPIE 4853* , 341–350 (2003).

[11] Shumko, S., Gorceix, N., Choi, S., Kellerer, A., Cao, W., Goode, P., Abramenko, V., Richards, K., Rimmele, T., and Marino, J., "Ao-308: the high-order adaptive optics system at Big Bear Solar Observatory," *Proc. SPIE 9148, id. 914835 11* (2014).

[12] Bonnefond, S., Tallon, M., Le Louarn, M., and Madec, P.-Y., "Wavefront reconstruction with pupil fragmentation," *Proc. SPIE 9909-287* (2016).
[13] Gisler, D., Berkefeld, T., and Berdyugina, S., "Planet imaging polarimetry with the solar telescope GREGOR," *Proc. SPIE 9906-206* (2016).
[14] Schmidt, D., B., T., Heidecke, F., Fischer, A., von der Lühe, O., and Soltau, D., "GREGOR MCAO looking at the Sun," *Proc. SPIE 9148, , id. 91481T 7* (2014).
[15] Schmidt, D., Gorceix, N., Marino, J., Berkefeld, T., Rimmele, T., Zhang, X., Wöger, F., and Goode, P., "Progress in multi-conjugate adaptive optics at Big Bear Solar Observatory," *Proc. SPIE 9909-83* (2016).